

1 **Absolute abundance estimates from shallow water baited underwater camera surveys; a**
2 **stochastic modelling approach tested against field data**

3
4 K.M. Dunlop ^{a,*}, G.D. Ruxton ^b, E.M. Scott ^c, D.M. Bailey ^a

5
6 ^a Institute of Biodiversity, Animal Health and Comparative Medicine, University of Glasgow, Glasgow,
7 G12 8QQ, UK

8 ^b School of Biology, University of St Andrews, St Andrews, Fife, KY16 9TH, UK

9 ^c School of Mathematics and Statistics, University of Glasgow, Glasgow, G12 8QQ, UK

10
11 * Corresponding author current address. Monterey Bay Aquarium Research Institute, 7700 Sandholdt Road,
12 Moss Landing, CA 95039, USA, Tel.: +1 831 775 1773; fax: +1 831 775 1638.

13 *E-mail address:* kdunlop@mbari.org (K.M. Dunlop).

14
15 **Abstract**

16
17 Baited underwater cameras are becoming a popular tool to monitor fish and invertebrate populations within
18 protected and inshore environments where trawl surveys are unsuitable. Modelling the arrival times of
19 deep-sea grenadiers using an inverse square relationship has enabled abundance estimates, comparable to
20 those from bottom trawl surveys, to be gathered from deep-sea baited camera surveys. Baited underwater
21 camera systems in the shallow water environments are however, currently limited to relative comparisons of
22 assemblages based on simple metrics such as Max_N (maximum number of fish seen at any one time). This
23 study describes a stochastic simulation approach used to model the behaviour of fish and invertebrates
24 around a BUC system to enable absolute abundance estimates to be generated from arrival patterns.
25 Species-specific models were developed for the tropical reef fishes the black tip grouper (*Epinephelus*
26 *fasciatus*) and moray eel (*Gymnothorax* spp.) and the Antarctic scavengers; the asteroid (*Odontaster*
27 *validus*) and the nemertean worm (*Parbolasia corrugatus*). A sensitivity analysis explored the impact of
28 input parameters on the arrival patterns (Max_N, time to the arrival of the first individual and the time to
29 reach Max_N) for each species generated by the model. Sensitivity analysis showed a particularly strong link
30 between Max_N and abundance indicating that this model could be used to generate absolute abundances
31 from existing or future Max_N data. It in effect allows the slope of the Max_N vs. abundance relationship to be
32 estimated. Arrival patterns generated by each model were used to estimate population density for the focal
33 species and these estimates were compared to data from underwater visual census transects. Using a Bland-
34 Altman analysis, baited underwater camera data processed using this model were shown to generate
35 absolute abundance estimates that were comparable to underwater visual census data.

36
37 **Highlights:**

- 38 - Modelling the behaviour of fish and invertebrates around a baited camera system
39 - Models developed for tropical fish and Antarctic invertebrates
40 - Abundance estimates calculated and compared to data from visual census transects

41 - Comparable abundance estimates generated by the model and transects

42 **Keywords:** baited underwater cameras; modeling; fish and invertebrate surveys; underwater visual census

43

44 **Abbreviations:**

45 BUC: Baited underwater camera

46 Max_N : Maximum number of individuals, of the same species, appearing on the field of view in any one
47 frame over the whole deployment

48 $T_{arrival}$: Time to the arrival of the first individual from each species

49 T_{maxN} : Time to the maximum number of individuals observed at one time

50 UVC: Underwater visual census

51

52 **1. Introduction**

53

54 Abundance estimates of marine populations, that are both accurate, close to the true abundance, and
55 precise, repeatable under the same conditions, are important to understand changes in marine populations or
56 communities (Farnsworth et al., 2007) and to help achieve sustainable management and effective
57 conservation objectives (Collins et al., 2002). For marine fish and invertebrate populations the majority of
58 this data has been collected using trawl surveys (Fitzpatrick et al., 2012; Johnson et al., 2012), which are
59 difficult in abyssal environments and unsuitable in marine protected areas (Bailey et al., 2007). Baited
60 underwater camera (BUC) systems have therefore been used in many studies to gather data on deep-sea
61 scavenging fauna (Farnsworth et al., 2007) and fish assemblages in protected areas (Willis and Babcock,
62 2000; McLean et al., 2010). However, to use BUC data to produce absolute abundance estimates of fish
63 and invertebrate populations requires a detailed understanding of the physical and biological parameters
64 involved in the process of animals detecting and following the bait plume to the camera (Priede et al., 1994;
65 Bailey et al., 2007).

66

67 Bait plume dispersal from a point source, its detection by fish or invertebrates and their arrival at the
68 source, is influenced by a number of environmental and biological factors (Collins et al., 2002; Stoner,
69 2004). The odour from the bait disperses as a plume into the surrounding water on currents (Reidenbach
70 and Koehl, 2011). The velocity and direction of currents will affect the length and lateral dispersal of the
71 plume as well as its dispersal direction (Bailey and Priede, 2002; Dorman et al., 2012). The dispersal of
72 odour plumes is also affected by turbulence within the aquatic environment (Meager and Batty, 2007), the
73 topography over which it travels (Collins et al., 1999; Collins et al., 2002; Reidenbach and Koehl, 2011) and
74 the characteristics and persistence of the bait (Bailey and Priede, 2002; Stoner, 2004). Fish and
75 invertebrates have evolved olfactory organs with chemosensory abilities that allow them to detect odour
76 plumes and follow them to their source (Reidenbach and Koehl, 2011). The area within the odour plume
77 where the odour concentration is above the threshold which organisms can detect is known as the 'active
78 space' (Sigler, 2000; Stoner, 2004). The probability of the fish entering the active space of the bait plume
79 will be dependent on their search behaviours (Dorman et al., 2012), including their swimming speed and
80 position in the water when foraging (Stoner, 2004), as well as the abundance and distribution of the

81 population (Armstrong et al., 1992). Once the plume has been detected, the fish will decide whether to
82 follow it based on the feeding motivation that the bait provides (Dorman et al., 2012). The time that
83 individuals remain at the bait will be determined by the availability of food within the environment
84 (Charnov, 1976) as well as the competition and interactions with other scavengers at the bait (Armstrong et
85 al., 1992; Bailey and Priede, 2002; Dunlop et al., 2014).

86

87 The process of bait plume detection, attraction and arrival of the deep sea grenadier *Coryphaenoides*
88 *armatus* at a BUC was modelled using an inverse square relationship:

89

$$90 \quad n = c/t_{\text{arr}}^2$$

91

92 where n is the number of fish per square kilometre and c is a constant, dependent upon the current velocity
93 and through water swimming speed of the fish towards the BUC system (Priede et al., 1990; Priede and
94 Bagley, 2000). t_{arr} represents the time elapsed between the beginning of the camera deployment and the
95 arrival of the first fish. The model was developed by Priede et al., (1990) to allow scavenger density to be
96 estimated from their arrival rates at the BUC in conjunction with information on the odour plume spreading
97 characteristics, current velocities and fish swimming speed. The staying time of deep-sea grenadiers at the
98 BUC can be estimated using the relationship:

99

$$N_{\beta} = \frac{\alpha_0}{x}(1 - e^{-\beta x})$$

100

101 where N_{β} is the maximum number of fish present after a certain period of time, α_0 the initial rate of fish
102 arrival at time zero, e the exponential constant and x a constant representing the decay of the odour plume
103 from dilution and bait consumption (Priede et al., 1990). Arrival rates are of interest as a bait placed
104 amongst an abundant scavenger population has a greater chance of being reached by an individual quickly
105 (Bassett and Montgomery, 2011). The arrival times of deep-sea grenadiers at a BUC in two sites in the
106 North Atlantic were modelled in the above manner to produce estimates of abundance which were
107 comparable to those from bottom trawl surveys from approximately the same area and time (Armstrong et
108 al., 1992; Priede and Merrett, 1996). However, when applied to fish arrival times on the Mid-Atlantic Ridge
109 there was no correlation between BUC generated abundances and those estimated from trawls (Bailey et al.,
110 2007).

111

112 The use of BUC systems in shallow waters have enabled relative comparisons of both fish and
113 invertebrate assemblages in the tropical (McLean et al., 2010; Moore et al., 2010), temperate (Willis et al.,
114 2003) and the Antarctic environments (Smale et al., 2007) between areas of different protection status
115 (Willis and Babcock, 2000; Westera et al., 2003), habitat type (Moore et al., 2010) and disturbance pressure
116 (Smale et al., 2007). The majority of studies have used the maximum number of individuals, of the same
117 species, appearing in the field of view in any one frame over the whole deployment (Max_N) as an index of
118 relative abundance (Willis and Babcock, 2000; Stoner et al., 2008). Max_N avoids the repeated recording of
119 individuals that leave and re-enter the camera field of view and usually less than the count of all animals

120 visiting the bait (McLean et al., 2010; Harvey et al., 2012). Some surveys have also used the time to the
121 arrival of the first individual from each species (t_{arrival}) and time to the maximum number of individuals
122 observed at one time (t_{maxN}) (Willis and Babcock, 2000; Jones et al., 2003). In the shallow water
123 environment however, the development of models of the process of fish or invertebrate arrival at BUCs has
124 been limited (Stoner et al., 2008; Langlois et al., 2012). Heagney et al., (2007) investigated whether abyssal
125 scavenger arrival models could be applied to shallow mid-water baited underwater video data. Existing
126 models appropriate for deep-sea BUC studies with long soak times and where scavengers approached more
127 slowly, were found unsuitable for shallow water BUC studies with much shorter soak times and which
128 attract many fast moving species (Heagney et al., 2007). Rapid arrival patterns of shallow water fish result
129 in overestimated abundance due to the inverse square law of the abyssal model (King et al., 2006; Stobart et
130 al., 2007). Compared to the shallow water environment, currents in the abyss are relatively constant, so an
131 assumption of a constant current speed and direction is more suitable (Heagney et al., 2007; King et al.,
132 2008). The assumptions of deep-sea models also cannot be applied to describe the foraging behaviours of
133 shallow water fish species, which also use sight, as well as chemoreception, to find food (Ellis and
134 DeMartini, 1995; Stobart et al., 2007). The time related metrics used in the deep-sea such as, t_{arrival} and t_{maxN} ,
135 have not correlated well with other surveys methods in some shallow water BUC surveys (Stoner et al.,
136 2008; Willis and Babcock, 2000).

137

138 The area sampled by the active space of the odour plume is largely unknown in shallow BUC surveys.
139 Concerns have been raised regarding the effect of localised environmental conditions, such as topography
140 and current conditions, on plume dynamics making it difficult to make comparisons between areas (Taylor
141 et al., 2013; Watson et al., 2009). Surveys assume that a comparable area is sampled by each deployment,
142 however, this will often be untrue if current conditions vary (Heagney et al., 2007). The importance of the
143 currents on the dynamics of bait plume dispersal and subsequent fish arrival patterns have been highlighted
144 in several studies in the mid water (Heagney et al., 2007) and demersal environments (Dorman et al., 2012).
145 The unknown sample area of shallow water BUC surveys also makes it difficult to make comparisons with
146 abundance estimates from other survey methods. Several studies have investigated the differences in fish
147 and invertebrate studies recorded by BUC and UVC surveys (Langlois, 2006; Watson et al., 2010),
148 however, conclusions regarding comparisons have been difficult as the area sampled cannot be directly
149 compared (Langlois et al., 2010).

150

151 A model to determine the absolute measures of shallow water fish or invertebrate abundance from
152 arrival patterns at a BUC would involve developing an area based bait dispersion model using in-situ
153 measurements of current speed and direction (Heagney et al., 2007). The mechanistic models outlined by
154 Priede et al., (1990) to estimate the abundance of deep-sea demersal fish from first arrival times are
155 deterministic. However, the arrival rate of fish is stochastically related to population abundance and the
156 factors governing aspects of shallow water fish movement are often assumed to be well represented by
157 random distribution (Farnsworth et al., 2007). This means it is important to include stochastic elements to
158 mechanistic models. The physical factors, current distribution and velocity, observed around the camera
159 system also have a random distribution within a particular range. Therefore it is important to introduce this

160 random aspect into models to describe fish attraction and arrival at a BUC system. Stochastic models that
 161 incorporate both the predictable and random aspects of a process, are increasingly being used to build our
 162 understanding of complex natural ecosystems (Brown and Kulasiri, 1996). Farnsworth et al., (2007) also
 163 modelled the arrival process of deep-sea demersal scavengers at the BUC using the addition of stochastic
 164 elements to deterministic models. Farnsworth's (2007) models unfortunately did not include a mechanism
 165 to reverse the process and calculate abundances from arrival patterns. The models also required a very large
 166 number of assumptions and parameters, making them difficult to implement for many BUC users.

167

168 The primary objective of the present study was to develop a stochastic modelling approach to enable the
 169 estimation of the absolute abundance of fish and invertebrates using arrival data collected using a shallow
 170 water BUC system. This involved the development of species-specific models for two fish and two
 171 invertebrate species observed in tropical and Antarctic BUC surveys. A global sensitivity analysis was used
 172 to determine the impact of model parameters on the arrival pattern produced by the model. A secondary
 173 objective, following the development of an effective modelling methodology, was to demonstrate how
 174 absolute abundance estimates can be generated from BUC data using the methodology. The achievement of
 175 this objective was assessed by comparing the model absolute abundance outputs to those from
 176 corresponding underwater visual census (UVC) transects. It was hypothesised that 1), the sensitivity
 177 analysis would show which model variables have an effect upon the arrival pattern of fish or invertebrates at
 178 the BUC and what aspects of the arrival pattern variable are affected the most (i.e. Max_N , t_{arrival} and t_{maxN})
 179 and 2), that the modelling methodology would generate absolute abundance estimate that were comparable
 180 to those from corresponding UVC surveys.

181

182 2. Materials and Methods

183

184 2.1. Model outline

185

186 The simulation was built in MATLAB (R2010b) using the movement of an individual fish around a
 187 BUC system within a designated area. A bait plume was plotted and the area covered (B_a , m^2) was
 188 described as a sector of a circle, using the three equations below. The length of the plume (L_{pl} , m) was
 189 calculated using a radius described as the mean current speed (V_w , ms^{-1}) recorded throughout the
 190 deployment multiplied by the simulation time (T , seconds). The plume therefore expanded with every time
 191 step of the simulation. The plume angle (Pl_{θ} , radians) was calculated from the inverse tangent of the
 192 diffusional velocity (B_y , ms^{-1}), divided by the current speed (V_w , ms^{-1}). The relationship between these
 193 model parameters is described in the equations:

$$L_{pl} = V_w T$$

$$Pl_{\theta} = 2 \tan^{-1} \left(\frac{B_y}{V_w} \right)$$

$$B_a = \left(\frac{\theta}{2} \right) L_{pl}^2$$

194 Simulations depict the movement of a population of a fixed abundance within a defined area (A , m^2). Prior
 195 to detection of the bait plume fish move at a cruising speed (V_{cr} , ms^{-1}) or are stationary, and turned a random

196 number of times (T_r) within a set time period known as the turning interval (Int_{tr} , seconds). The direction
 197 within which the fish travels after each turn (D_r , radians) was randomly selected (independently for each
 198 individual).

199

200

$$D_r = rand(0, 360)$$

$$Int_{tr} = rand(0, T_r) * T_r$$

201

202 The starting point ($P_{st}(x, y)$) was selected (again independently for each individual) from a random
 203 position within the simulation area (A , m^2) using the formula below:

204

$$(P_{st}(x, y)) = rand\left(-\frac{A}{2}, \frac{A}{2}\right)$$

205

206 The distance travelled per time step (D_s , m) was calculated by dividing the cruising speed by the time
 207 resolution (T_r , seconds). Distance travelled in the x and y axis ($D_s(x, y)$) was found by multiplying the
 208 cruise speed divided by the simulation time resolution (length of the time-step used in simulations) and
 209 multiplying this by sine and cosine of the direction (D_r , radians):

210

211

$$D_s(x) = \frac{V_{cr}}{T_r} \sin(D_r)$$

212

$$D_s(y) = \frac{V_{cr}}{T_r} \cos(D_r)$$

213

214 The distance to the camera ($D_{cm}(x, y)$) was calculated by taking the square root of the distance travelled in
 215 the x and y axis:

$$D_{cm}(x, y) = \sqrt{D_s(x, y)^2}$$

216

217 When the distance to the camera ($D_{cm}(x, y)$) is less than the radius associated with the circular bait area
 218 (B_a , m^2) the fish is considered to have encountered the bait plume area. On encounter the fish turns into an
 219 approach angle $app(\theta)$ calculated using:

220

$$app(\theta) = (180, 360, 0, -180 \tan^{-1} D_s\left(\frac{x}{y}\right))$$

221

222 (the angle used in this equation depends upon the position on the fish when the bait plume is encountered).

223 This change in direction causes the fish to swim directly upstream towards the bait at a through-water

224 approach speed up the plume towards the camera ($V_{f_{sa}}$, ms^{-1}). This speed is faster than the cruising

225 swimming speed and was calculated from observation of fish max swimming speed in previous published

226 studies. Current speed (V_w , ms^{-1}) is subtracted to account for the fish swimming upstream against the

227 current. Once in the bait plume the distance travelled towards the camera and its relation to the camera

228 position is recalculated using the through-water approach speed ($V_{f_{sa}}$, ms^{-1}):

229

230
$$D_s(x) = \frac{V_{f_{sa}}}{T_r} \sin(D_r)$$

231
$$D_s(y) = \frac{V_{f_{sa}}}{T_r} \cos(D_r)$$

232

233 Upon reaching the bait the individual will remain there for a “staying time” (S_t , seconds) found by taking a
 234 random time between a pre-determined interval. This was multiplied by the time resolution (T_r , seconds) of
 235 the simulation:

$$S_t = rand([1800, T_r])$$

236

237 After remaining at the camera for the staying time the fish is removed from the simulation as it is assumed
 238 to have reached satiation or decided to forage elsewhere. Simulations run for 60 or 90 minutes and record
 239 the total number of fish, or invertebrates, present at the bait every 30 seconds, the same interval is used in
 240 the in-situ BUC studies. For the invertebrates studied here staying time was set till the simulation end. The
 241 model is depicted in as a diagram in Fig. 1.

242

243 2.2. General assumptions

244

245 Fish or invertebrates are assumed to act independently of each other at all stages of the simulation and to
 246 always react to the bait plume on encounter. The bait plume was always spread from the origin of the
 247 coordinate system used in the simulations and assumed to disperse in a single direction. The present model
 248 assumes a constant plume concentration and represents a framework that can be combined with fluid
 249 dynamics models of bait plume dispersal from a point source in the future to enable the dilution of the
 250 plume concentration and changes in current direction to be incorporated into the models.

251

252 Simulations were developed for four species; the grouper *Epinephelus fasciatus* and moray eels of the
 253 genus *Gymnothorax* spp. recorded in the tropical Gulf of Aqaba and the Antarctic scavenging invertebrates
 254 *Odontaster validus* and *Parbolasia corrugatus*. The BUC system consisted of a digital stills camera
 255 (SeaLife DC800 or DC1000) enclosed in an underwater housing. No additional light was required for work
 256 in the Gulf of Aqaba, but in Antarctica the camera was synchronized, via optical cables, with two variable-
 257 power digital slave strobe light units (Epoque ES-23DS). The camera was placed in time lapse mode (30 s
 258 intervals). The camera equipment was supported on an L-shaped frame of aluminium tubing. A u-shaped
 259 bracket holding the camera was bolted to the vertical element of the frame and angled downwards at 60° to
 260 view the mesh bait bag attached to the far end of a horizontal pole. 200 g of either chopped fish (*Sparus*
 261 *aurata* and *Dicentrarchus labrax*) in the Gulf of Aqaba or chopped Antarctic invertebrates (*Ophionotus*
 262 *victoriae*, *O. validus*, *Sterechinus neumayeri* and *Laternula elliptica*) were used as bait. The system was
 263 deployed from a boat and lowered to the seabed or placed by a SCUBA diver. A ballast weight (c10kg) held
 264 the camera system to the seabed and it was held upright in the water column by two small mid-water buoys.
 265 At the end of deployments the camera system was recovered either by hauling on a recovery line or by
 266 attachment and inflation of a lifting bag by SCUBA divers.

267 Data on swimming or crawling speeds, the turning frequency and aspects of the foraging behaviours for
268 each species were determined from published studies (Fulton, 2007; D'Aout and Aerts, 1999; Clarke and
269 Prothero-Thomas, 1997; Kidawa, 2001; Bshary et al., 2006) (Table 1). Estimations of staying time were
270 based on observation of individuals in BUC deployments. For the tropical species it was difficult to identify
271 individuals to calculate their staying time at the bait and estimations were taken from observation of the
272 number of consecutive images an individual of that species was observed in. Current velocity was recorded
273 during Antarctic deployments using a Nortek Aquadopp Acoustic Doppler current meter (Aquadopp
274 Current Meter, Nortek, USA) while for the Gulf of Aqaba data an Acoustic Doppler Current Profiler
275 between 10 m and 1 km from BUC deployments was used. Current meter measurements provided the
276 current ranges within which the simulation could operate.

277 All BUC deployments had a matching underwater visual census (UVC) transect at the same location and
278 depth making up on station. In the Gulf of Aqaba an area of 100 m² was swum once (50 x 2 m transect) and
279 the numbers of *E. fasciatus* and *Gymnothorax* spp. were recorded on a slate (32 stations total, eight at each
280 at 5, 10, 15 and 20 m). In Antarctica the density of *O. validus* and *P. corrugatus* was recorded from
281 analysis of images from a 25 x 0.5 m UVC transect of continuous stills images (18 stations total, six each at
282 5, 10 and 25 m).

283

284 The ranges of input parameters for each model are described in Table 1. The current speeds observed
285 during the BUC deployments in both the Antarctic and the Gulf of Aqaba were approximately comparable
286 to the current speeds measured in the deep-sea environment by Sainte-Marie and Hargrave, (1987).
287 Therefore, due to the lack of measurements of the diffusional velocities the same velocity, 10⁻³ m s⁻¹, used to
288 model the arrival of scavengers at a baited camera by Sainte-Marie and Hargrave, (1987) was used.

289

290 Moray eels of the genus *Gymnothorax* and blacktip groupers (*E. fasciatus*) are ambush predators highly
291 associated with rocky reefs and crevices and will defend a small territory (Gibran, 2007). Therefore in
292 simulations of *Gymnothorax* spp. and *E. fasciatus* movement around the BUC system individuals were
293 relatively slow moving prior to the detection of the bait plume. Antarctic invertebrate scavengers are slow
294 moving compared to the tropical fish therefore BUC deployments in the shallow water Antarctic
295 environment lasted for 1.5 h. The invertebrates also crawl along the seabed so current velocity was not
296 subtracted from the approach velocity. Both Antarctic scavengers remained stationary prior to the detection
297 of an odour plume and on reaching the bait scavengers remained there till the end of the simulation as
298 observed in BUC deployments.

299

300 2.3. Data analysis

301

302 Models generated an arrival patterns for fish or invertebrates at the bait based on a predicted number
303 present every 30 s, to produce a dataset in the same form as that from in-situ BUC deployments. Max_N,
304 t_{arrival} and t_{maxN} were used to describe the arrival pattern of fish or invertebrates at the BUC. This sensitivity
305 analysis enabled the dependence of the fish or invertebrate arrival pattern output by the model on input
306 parameters to be determined and was used to test hypothesis one. A global sensitivity analysis was

307 performed on each species-specific model to determine the impact of the input parameters; population
308 abundance, current speed, diffusional velocity, swimming speed before contact with the odour plume,
309 approach speed and staying time (Table. 1). Each input parameter was set to be randomly selected from the
310 full range of potential values and each of the four models was run 300 times to ensure that the full range of
311 potential input parameters was considered. This was checked by plotting a histogram of the distribution of
312 the input parameters and was also used to ensure that the range of input values had a random distribution.
313 Both the marginal and bivariate simulated factor distributions were explored to ensure that coverage of the
314 factor space was extensive (Saltelli, 2000).

315

316 A stepwise regression was performed in R (version 3.0.2, The R Development Core Team, 2013) to
317 examine the relationship between the input parameters and the model output abundance indices; Max_N ,
318 $t_{arrival}$ and t_{maxN} . The relationship between any input parameter identified as having a significant effect on
319 Max_N , $t_{arrival}$ and t_{maxN} was plotted in a scatter plot. The relationship between the model parameters and the
320 BUC abundance indices were unknown as this early stage of model development and the stepwise
321 regression was used as a tool to explore these relationships. The analysis of the influence of model input
322 parameters on the resultant fish or invertebrate arrival pattern highlighted which parameters were important
323 to calibrate with in-situ measurements.

324

325 *2.4. Producing absolute abundance estimates from BUC data*

326

327 Any parameters with a significant effect were parameterised using an in-situ measurement of this
328 variable where available. For example, if current speed had a significant impact on the Max_N then the
329 current speed from the in-situ BUC deployment providing the camera data was used to produce an
330 abundance estimate was used as a model input. Those identified as having no significant impact on the
331 model output were set to be selected randomly from a range of suitable values for that measure. However,
332 for some parameters an in-situ measurement was not available and values within the models had to remain
333 as the estimates ranges. These parameters were highlighted as those requiring future measurement to
334 improve the accuracy of the model outputs.

335

336 To produce absolute abundance estimates using the modelling methodology a suitable range of estimated
337 population abundances must be first input into the model. In practice these estimates could be derived from
338 previous surveys using other methods, literature for similar areas or be best guesses. In the case of this
339 validation exercise corresponding UVC surveys from the same position and approximately the same time as
340 the BUC deployments were used to find a suitable abundance range for the tropical and Antarctic models.
341 Each single population abundance input into the model produced a BUC arrival pattern. For example, if an
342 abundance range of 1 - 100 individuals was used 99 arrival patterns would be produced. The arrival
343 patterns produced by the model were compared to the arrival patterns produced by the corresponding BUC
344 survey. The R-squared value of the slope fitted to the arrival curve of individuals at the camera with time
345 was used to find a match between model and BUC arrival patterns. Once a match was found the population
346 abundance input into the model to produce that arrival pattern is recorded as the model's best estimate of the

347 absolute abundance of the fish or invertebrate population surveyed by the BUC system. This process is
348 illustrated in Fig. 2 where the arrival pattern from five model runs of the model of *E. fasciatus* movement
349 around the BUC can be compared to that of the in-situ BUC arrival pattern.

350

351 The absolute abundance estimate produced using the model methodology and field BUC data were
352 compared to those generated by corresponding UVC surveys to validate the ability of the model to produce
353 accurate abundance estimates. Models describing the movement of the two tropical fish species and the two
354 Antarctic invertebrate scavengers in relation to the BUC system were validated using transect data. BUC
355 absolute abundance estimates were compared to those from the corresponding UVC surveys using a Bland-
356 Altman analysis (Bland and Altman, 1986). A Bland-Altman analysis is used to compare two methods of
357 measurement, usually a new method with an established one (Bland and Altman, 1986). In this study the
358 UVC represents the established method for measuring fish and invertebrate absolute abundance and the
359 BUC the new method. The Bland-Altman plots show the mean difference between the two corresponding
360 measurements from both methods, known as ‘the bias’, and the 95% limits of agreement as ± 1.95 SD of
361 the mean difference. The plot enables visual judgement of the agreement between the measurements and
362 the smaller the range between the measurements the better the match (Bland and Altman, 1986; Bland and
363 Altman, 1995). An analysis showing no significant systematic bias between the two methods would show
364 the majority of the data points within the confidence limits and that points would have a symmetrical around
365 zero. A Bland and Altman analysis was performed in the R package ‘MethComp’ and a Bland-Altman plot
366 and measures of the test bias test were produced to compare the measurements of absolute abundance using
367 the UVC and tropical and Antarctic BUC models (Fig. 3).

368

369 3. Results

370

371 3.1. Sensitivity analysis

372

373 The input parameters (abundance, current speed, approach speed, cruising speed, diffusional velocity
374 and staying time) produced by 300 runs of the 4 models were plotted in frequency histograms and their
375 distribution was random and encompassed the full range of potential input parameters. Sensitivity analysis
376 revealed that the model input parameters explained a large proportion of the variability in the Max_N output
377 of the 4 models. Input parameters explained less of the variability in the time-based metrics ($t_{arrival}$ and
378 t_{maxN}). Abundance was the model input parameter that had the greatest impact on the Max_N , $t_{arrival}$ and t_{maxN}
379 outputs from the model for all 4 species.

380

381 For both tropical models the parameter population abundance explained a large proportion of the
382 variability in the Max_N output; *E. fasciatus* ($y = 0.73x + 0.71$; R-sq (adj) = 91.74; $P < 0.0001$) and for
383 *Gymnothorax* spp. ($y = 0.57x + 0.49$; R-sq (adj) = 97.99; $P < 0.0001$). Input parameters explained less of
384 the variability in the $t_{arrival}$ of tropical fish at the bait. Population abundance had a small but significant
385 effect on *E. fasciatus* ($y = 61.81x + 217.89$; R-sq (adj) = 18.16; $P < 0.0001$) and *Gymnothorax* spp. $t_{arrival}$ (y
386 = $-54.21x + 83.89$; R-sq (adj) = 30.17; $P < 0.0001$). Current speed also had a significant impact on

387 *Gymnothorax. spp.* t_{arrival} ($y = 135.45x + 42.94$; R-sq (adj) = 1.47; $P = 0.02$). Current speed explained 1.8%
388 of the *Gymnothorax. spp.* t_{maxN} ($y = 315.57x + 191.45$; R-sq (adj) = 1.8; $P = 0.018$) and population
389 abundance had a significant impact on *E. fasciatus* t_{maxN} ($y = 1792.8x + 6614.5$; R-sq (adj) = 6.71%; $P <$
390 0.0001). Staying time had no effect upon indices for both tropical models.

391

392 Only population abundance input into models of the Antarctic asteroid *O. validus* movement around the
393 BUC explained a significant proportion of the Max_N values generated ($y = 0.53x - 0.92$; R-sq (adj) = 49.32;
394 $P < 0.0001$). *O. validus* t_{arrival} and t_{MaxN} values were also only significantly affected by input abundance ($y =$
395 $-234.17x + 5199.6$ and $y = -23.84 + 4915.4$; R-sq (adj) = 19.14 and 3.37; $P < 0.0001$ and $P = 0.0008$). For
396 *P. corrugatus* input abundance accounted for 34.48% of the variability in Max_N ($y = 0.2241 - 0.0985$; R-sq
397 (adj) = 34.4; $P < 0.0001$) and t_{arrival} and t_{maxN} 19.29% and 1.49% ($y = -163.74 + 4879.5$ and $y = -15.179 +$
398 4662.0 ; R-sq (adj) = 19.29 and 1.49; $P < 0.0001$ and $P = 0.03$). Current speed and *P. corrugatus* approach
399 speed had no significant effect upon Max_N , t_{arrival} and t_{maxN} values.

400

401 3.2. Comparison to baited underwater camera data

402

403 The Max_N output of the models developed to describe the behaviour of the two tropical fish and
404 Antarctic invertebrate species were all primarily affected by the input parameter population abundance.
405 Therefore, Max_N was only used to match arrival patterns from the in-situ BUC deployment and the multiple
406 model arrival patterns. T_{arrival} and t_{maxN} were also significantly related to abundance and could also be
407 potentially used to select model arrival patterns. There was limited evidence from the sensitivity analysis of
408 the effect of the other model parameters on the model abundance indices therefore parameters were kept
409 within the ranges reported in Table 1.

410

411 For 10 of the BUC deployments the corresponding UVC recorded no groupers and for three of the UVC
412 transects that observed groupers none were observed in corresponding BUC deployments. 10
413 corresponding UVC and BUC pairs both recorded *E. fasciatus* and for 9 of these pairs the BUC model
414 produced the same or slightly higher abundance estimates (Fig. 3a). The Bland Altman plot provides little
415 evidence of systematic bias between the abundance estimates of the grouper *E. fasciatus* generated by the
416 BUC model methodology and the UVC surveys. This is concluded as all data points are within the +/- 1.96
417 SD limits of agreement in the plots and points are distributed symmetrically around the mean (Fig.4a). Only
418 4 corresponding UVC and BUC pairs both observed moray eels of the genus *Gymnothorax* and the BUC
419 model produced higher or the same abundances. Moray eels were only observed in BUCs in 8 of the
420 corresponding UVC and BUC pairs and only in UVC in 4 pairs. The Bland-Altman plot show that points
421 are symmetrically distributed around the mean and that all point were within the +/- 1.96 SD limits of
422 agreement (Fig.4b).

423

424 In all 18 UVC and BUC pairs *O. validus* was observed and there was no clear pattern of differences
425 between the abundance estimates recorded by each method (Fig.3c). All the data points for *O. validus*
426 abundance estimates from the BUC model and the UVC were within or on the +/- 1.96 SD limits of

427 agreement. From the plot it would however, appear that the plots were slightly asymmetrical to the zero and
428 that average abundances from the model are slightly less than those recorded by the UVC as the abundance
429 of *O. validus* increases (Fig.4c). For 8 of the 18 corresponding transect and BUC model pairs abundance
430 estimates for *P. corrugatus* were only recorded by the BUC model and in a further 6 pairs the BUC model
431 estimates were much larger than in the UVC surveys (Fig.3d). In the Bland-Altman plots two outliers were
432 removed where abundances > 100 individuals were recorded by the BUC. All points were within the 1.96
433 SD limits of agreement but they were not symmetrically distributed around the mean indicating that higher
434 abundances were measured by the BUC (Fig.4d).

435

436 **4. Discussion**

437

438 Results from the sensitivity analysis indicate that for tropical and Antarctic models of fish and
439 invertebrate movement around the BUC system the abundance of the surveyed population was the factor
440 most strongly related to the Max_N. These models allow a BUC user to determine the relationship between
441 Max_N and the abundance of the focal species and allow the commonly collected Max_N unit of relative
442 abundance to be converted to absolute units. Two other commonly-recorded indices of abundance, t_{arrival}
443 and t_{maxN} appear to be less closely related to absolute abundance than might have been assumed, but might
444 usefully contribute to model parameter selection where more than one abundance value results in the
445 observed Max_N. Within the range of species used here, estimates of their searching speed and staying time
446 had relatively little influence on the model Max_N. This is a reassuring finding as it is relatively difficult to
447 estimate these behavioural values in wild animals.

448

449 For all species-specific, models Max_N appeared to be the measure which accounted for most of the
450 variability in the input population abundance fish or invertebrates. Measurements of t_{arrival} and t_{maxN} would
451 however, reflect more about aspects of fish approach swimming speed and the current velocity observed
452 around the BUC deployment. Stoner et al., (2008) found that a poor correlation exists between BUC time
453 based metrics and abundance estimates of juvenile Pacific cod from corresponding seine net trawls, while
454 Max_N measures correlated well with trawl survey results. Time based metrics from BUC studies in the
455 abyssal environment have however, been used successfully to calculate the absolute abundance of
456 scavenging fish populations (Priede and Merrett, 1996). The current speeds observed around the BUC
457 deployments and that were used for model ranges were relatively slow. If BUC deployments were within
458 environments experiencing high current speeds then possibly variation in current speed would likely have a
459 greater affect on BUC output indices and detailed current speed measurements during BUC deployments
460 would be essential. The model framework presented here allows these different scenarios to be tested
461 against field data. Estimates of the range of diffusional velocities experienced in the tropical and Antarctic
462 environments were not available to investigate its potential effect upon arrival patterns, but again the
463 framework allows easy incorporation of new field or laboratory data on diffusion to be incorporated as it
464 becomes available. The incorporation of fluid dynamics modelling into the methodology would enable the
465 potential effects of current speed and diffusional velocity on the arrival of fish or invertebrates at the BUC
466 to be explored in more detail. Unlike previous models an odour plume of any shape or concentration can be

467 incorporated into this framework to replace the “pie segment” used here. Animals contacted by the plume or
468 walking/swimming into the side of it would respond in the same way as those in the existing models.
469 Refinements such as animals resuming random movement if they leave an irregularly shaped plume would
470 be added at this stage.

471

472 Staying time had no impact on abundance metrics even though it had been shown to affect Max_N values
473 in the deep-sea BUC studies (Priede et al., 1990). The majority of BUC studies in the abyssal northeast
474 Atlantic found the mean staying time of the deep-sea grenadier (*C. armatus*) to be approximately 2 hours
475 (Priede et al., 1994; Henriques et al., 2002). In the shallow water BUC fish arrive more rapidly and
476 frequently, causing the staying time to likely have less of an impact on Max_N values. With longer staying
477 times the number of fish at the camera will accumulate to reach Max_N and the total meaning that Max_N will
478 have more of a linear relationship with the numbers visiting the BUC. However, in the shallow water
479 environment where more fish are coming and going from the field of view there maybe a larger difference
480 between Max_N and the total number of animals visiting the camera. These results therefore indicate that in
481 these models accurate estimate of fish or invertebrate staying time, cruising speed or diffusional velocity are
482 not important to the output of the model and therefore all that is necessary is the selection of a suitable
483 range. More important factors such as fish and invertebrate approach speed and the current speed should be
484 prioritised. The latter is certainly directly measurable at the camera, though in complex habitats the current
485 experienced by the fauna might be quite different. Approach speed is harder to ascertain, though stereo
486 camera systems such as BRUVS can probably provide useful information if the system lands facing
487 downstream at the point at which animals arrive. With downward-looking cameras the field of view is often
488 too small to get good estimates of movement speed, but not impossible, especially for slow-moving species.
489 In our Antarctic studies we were able to directly measure invertebrate walking speed across the seabed.

490

491 The absolute abundance estimates of *E. fasciatus* and *O. validus* generated by the BUC model
492 methodology were found to be most comparable to the abundance estimates from corresponding UVC
493 surveys. This is because these species are visible to the UVCs as well as to the BUC. The other two species
494 tend to be hidden in rocks (Clarke and Prothero-Thomas, 1997) or within the coral reef (Bshary et al., 2006)
495 except when bait is present, with their occasional appearance in the open probably being caused by recent
496 feeding or disturbance. Moray eels of the genus *Gymnothorax* are generally nocturnal hunters and during
497 the day they will remain hidden within rocky refuge (Bshary et al., 2006; Bardach et al., 1959) making it
498 difficult for daytime UVC surveys to detect them. In a number of BUC and UVC corresponding pairs the
499 BUC survey observed moray eels when the UVC surveys recorded none causing the BUC model to estimate
500 abundances when the UVC estimate equalled zero. The abundance estimates generated by the BUC models
501 for the nemertean worm *P. corrugatus* were higher than those within the higher abundance estimates were
502 produced by the BUC models for *P. corrugatus* due to the BUC recording *P. corrugatus* but none being
503 observed in the corresponding UVC survey. This can be attributed to the species taking refuge under rocks
504 during the day (Clarke et al., 1997) causing few to be observed in daytime transects. This will result in the
505 model parameters being calibrated to artificially low populations densities. Little is known about the
506 behaviour of *P. corrugatus* and it is possible that large groups of individuals congregate within refuges

507 (Clarke and Prothero-Thomas, 1997), violating the assumption of the model that individuals are randomly
508 distributed and act independently of each other.

509

510 Models also assume that all fish react and follow the bait plume once encountered, however factors such
511 as satiation state, olfactory capabilities and the availability of other food sources in the environment will
512 impact upon their decision. Due to the comparability of absolute abundance estimates from the BUC model
513 and the UVC, it would appear that a large proportion of the nearby animals from these species reacted to the
514 bait plume. Model assumptions include that individuals react independently of each other however,
515 competitive behavioural interactions have been observed to occur between fish at the bait of BUC systems
516 (Armstrong et al., 1992; Stoner et al., 2008; Dunlop et al., 2014). It has been suggested that these
517 interactions discourage some fish from approaching the bait due to the increased chance of competition
518 (Jones et al., 2013; Willis et al., 2003; Cappo et al., 2004) or predation (Lampitt et al., 1983; Harvey et al.,
519 2007) presented by the other fish. It is therefore evident that in both the fish species studied competitive
520 interactions around the BUC could potentially impact upon the arrival patterns of individuals at the bait.
521 The effect of other species interactions on the arrival patterns of fish and invertebrates at the BUC should
522 also be considered. Effects may include particular species posing a higher predation risk at the bait
523 reducing the number of the other species observed. Further studies of the impact of these interactions would
524 allow this information to be added to modelling approaches. Unlike previous models our framework would
525 allow multiple species models to be combined using information on the species composition and potentially
526 the effects of interactions on bait approach and staying times. Also when foraging individuals become close
527 to the bait they are potentially attracted by the movement and sounds of others feeding (Bailey and Priede,
528 2002). For shallow water fish species that rely heavily upon sight for foraging and hunting (Stoner et al.,
529 2008) this has the potential to impact on their behaviour in relation to the BUC system and thus arrival
530 patterns. Further valuable research would be the investigation of the application of this modelling approach
531 to other marine species, which have been found to be attracted to BUC systems. This would primarily
532 include the large, predatory mobile species that BUC surveys have been found to effectively survey
533 (Malcolm et al., 2007; Watson et al., 2010).

534

535 Preliminary results show that this stochastic modelling approach can generate absolute abundance
536 estimates of some shallow water fish and invertebrate populations from BUC deployments and that these
537 estimates are comparable to an established survey method. Discrepancies were apparently due to cryptic
538 behaviour in some species resulting in underestimates of abundance during underwater visual census
539 surveys. The generation of absolute abundance estimates from shallow BUC surveys improves the
540 application of the method substantially and makes the results comparable to those of other survey methods,
541 such as trawl surveys and transects commonly used in stock assessments and monitoring programmes. This
542 also enables previously-collected BUC data to be reanalysed and diversity indices for these deployments to
543 be recalculated based on the abundances of the animals present rather than combinations of Max_N values.

544

545 In conclusion, the spatial, stochastic modelling approach described and tested in this study represents
546 one of the first attempts to model the arrival process of shallow water marine species at a BUC system.

547 Initial results for a small set of tropical and Antarctic species-specific models show that this method has the
548 potential to generate absolute abundance estimates from BUC data that are comparable to UVC data. The
549 model could be used retrospectively to re-analyse existing Max_N data. This development combined with the
550 existing ability of BUCs to generate data in a time-and-cost efficient and non-destructive manner can
551 significantly improve the value of this method to monitor inshore marine populations.

552

553

554 **Figure and Table Legends**

555

556 **Fig. 1.** Diagram illustrating the general input and output parameters of the model simulation describing the
557 behaviour of fish and invertebrate populations in relation to a baited underwater camera system.

558

559 **Fig. 2.** Example plot of the arrival pattern of the black tip grouper (*Epinephelus fasciatus*) at the baited
560 underwater camera system (BUC) produced by 5 model runs and the arrival pattern from an in-situ BUC
561 deployment.

562

563 **Fig. 3.** Histograms and scatter plots comparing the absolute abundance estimates generate from UVC transects
564 (open bars) and BUC models (closed bars) for a) the grouper (*Epinephelus fasciatus*), b) the moray eel species
565 (*Gymnothorax* spp.), c) the Antarctic asteroid (*Odontaster validus*) and d) the Antarctic nemertean worm
566 (*Parbolasia corrugatus*).

567

568 **Fig. 4.** Bland Altman plots illustrating the agreement between the abundance estimates generated by the
569 baited underwater camera model (BUC) and the underwater visual census survey (UVC) for a) *Epinephelus*
570 *fasciatus*, b) *Gymnothorax* spp., c) *Odontaster validus* and d) *Parbolasia corrugatus*.

571

572 **Table 1** Input parameters ranges for *Epinephelus fasciatus*, *Gymnothorax* spp., *Pollachius virens*,
573 *Scyliorhinus canicula*, *Odontaster validus* and *Parbolasia corrugatus*.

574

575 **Acknowledgements**

576

577 This research was supported by a University of Glasgow Faculty Scholarship to KMD, a Collaborative
578 Gearing Scheme grant from the Natural Environmental Research Council and the British Antarctic Survey
579 and an ASSEMBLE infrastructure access grant to DMB. The authors would like to thank the staff of the
580 Inter-University Institute of Marine Sciences (IUI), Eilat, in particular Asaph Rivlin, Oded Ben-Shaprut and
581 Simon Berkowitz, and the diving and boating teams at Rothera Research Station, Western Antarctic
582 Peninsula, in particular Dr David Barnes and Ashley Cordingley. Permits were received from the Israel
583 Nature and Parks Agency and the authors thank both organisations for allowing us to conduct this work.

584 **References**

585

586 Armstrong, J.D., Bagley, P.M., Priede, I.G., 1992. Photographic and acoustic tracking observations of the
587 behaviours of the grenadier *Coryphaenoides (Nematoburus) armatus*, the eel *Synaphobranchus bathybius*,
588 and other abyssal demersal fish in the North Atlantic Ocean. Mar. Biol. 112, 535-544.

589 Bailey, D.M., Priede, I.G., 2002. Predicting fish behaviour in response to abyssal food falls. Mar. Biol. 141, 831-
590 840.

591 Bailey, D.M., Wagner, H.J., Jamieson, A.J., Ross, M.F., Priede, I.G., 2007. A taste of the deep-sea: The roles of
592 gustatory and tactile searching behaviour in the grenadier fish *Coryphaenoides armatus*. Deep. Sea. Res.
593 54, 99-108.

594 Bardach, J.E., Winn, H.E., Menzel, D.W., 1959. The role of the senses in the feeding of the nocturnal reef predators
595 *Gymnothorax moringa* and *G. vicinus*. Copeia 1959, 133-139.

596 Bassett, D.K., Montgomery, J.C., 2011. Investigating nocturnal fish populations *in situ* using baited underwater
597 video: With special reference to their olfactory capabilities. J. Exp. Mar. Biol. Ecol. 409, 194-199.

598 Bland, J.M., Altman, D.G., 1986. Statistical methods for assessing agreement between two methods of clinical
599 measurement. The Lancet 327, 307-310.

600 Bland, J.M., Altman, D.G., 1995. Comparing methods of measurement: why plotting difference against standard
601 method is misleading. The Lancet 346, 1085-1087.

602 Brown, T.N., Kulasiri, D., 1996. Validating models of complex, stochastic, biological systems. Ecol. Model. 86,
603 129-134.

604 Bshary, R., Hohner, A., Ait-el-Djoudi, K., Fricke, H., 2006. Interspecific communicative and coordinated hunting
605 between groupers and giant moray eels in the Red Sea. Plos. Biol. 4, e431.

606 Cappel, M., Speare, P., De'ath, G., 2004. Comparison of baited remote underwater video stations (BRUVS) and
607 prawn (shrimp) trawls for assessments of fish biodiversity in inter-reefal areas of the Great Barrier Reef
608 Marine Park. J. Exp. Mar. Biol. 302, 123-152.

609 Charnov, E.L., 1976. Optimal foraging, the marginal value theorem. Theor. Popul. Biol. 9, 129-136.

610 Clarke, A., Prothero-Thomas, E., 1997. The influence of feeding on oxygen consumption and nitrogen excretion in
611 the Antarctic nemertean *Parborlasia corrugatus*. Physiol. Biochem. Zool. 70, 639-649.

612 Collins, M. A., Yau, C., Nolan, C. P., Bagley, P. M., Priede, I. G., 1999. Behavioural observations on the scavenging
613 fauna of the Patagonian slope. J. Mar. Biol. Assoc. UK. 79, 963-970.

614 Collins, M.A., Yau, C., Guilfoyle, F., Bagley, P., Everson, I., Priede, I., Agnew, D., 2002. Assessment of stone crab
615 (Lithodidae) density on the South Georgia slope using baited video cameras. Ices. J. Mar. Sci. 59, 370-379.

616 D'Aout, K., Aerts, P., 1999. A kinematic comparison of forward and backward swimming in the eel *Anguilla*
617 *anguilla*. J. Exp. Biol. 202, 1511-1521.

618 Dorman, S.R., Harvey, E.S., Newman, S.J., 2012. Bait effects in sampling coral reef fish assemblages with stereo-
619 BRUVs. Plos One 7, e41538.

620 Dunlop, K.M., Scott, E.M., Parsons, D., Bailey, D.M., 2014. Do agonistic behaviours bias baited remote underwater
621 video surveys of fish? Mar. Ecol. (in press).

622 Ellis, D., DeMartini, E., 1995. Evaluation of a video camera technique for indexing abundances of juvenile pink
623 snapper, *Pristipomoides filamentosus*, and other Hawaiian insular shelf fishes. Fishery B-NOAA 93, 67-77

624 Farnsworth, K.D., Thygesen, U.H., Ditlevsen, S., King, N.J., 2007. How to estimate scavenger fish abundance using
625 baited camera data. Mar. Ecol. Prog. Ser. 350, 223-234.

- 626 Fitzpatrick, B.M., Harvey, E.S., Heyward, A.J., Twigg, E.J., Colquhoun, J., 2012. Habitat specialization in tropical
627 continental shelf demersal fish assemblages. *Plos One* 7, e39634.
- 628 Fulton, C.J., 2007. Swimming speed performance in coral reef fishes: field validations reveal distinct functional
629 groups. *Coral Reefs* 26, 217-228.
- 630 Gibran, F. Z., 2007. Activity, habitat use, feeding behavior, and diet of four sympatric species of Serranidae
631 (Actinopterygii: Perciformes) in southeastern Brazil. *Neotrop. Ichthyol.* 5, 387-398.
- 632 Harvey, E.S., Cappo, M., Butler, J.J., Hall, N., Kendrick, G.A., 2007. Bait attraction affects the performance of
633 remote underwater video stations in assessment of demersal fish community structure. *Mar. Ecol. Prog. Ser.*
634 350, 245-254.
- 635 Harvey, E.S., Newman, S.J., McLean, D.L., Cappo, M., Meeuwige, J.J., Skepperb, C.L., 2012. Comparison of the
636 relative efficiencies of stereo-BRUVs and traps for sampling tropical continental shelf demersal fishes.
637 *Fish. Res.* 125, 108-120.
- 638 Heagney, E.C., Lynch, T.P., Babcock, R.C., Suthers, I.M., 2007. Pelagic fish assemblages assessed using mid-water
639 baited video: Standardising fish counts using bait plume size. *Mar. Ecol. Prog. Ser.* 350, 255-266.
- 640 Henriques, C., Priede, I.G., Bagley, P.M., 2002. Baited camera observations of deep-sea demersal fishes of the
641 northeast Atlantic Ocean at 15-28 degrees N off West Africa. *Mar. Biol.* 141, 307-314.
- 642 Johnson, A.F., Jenkins, S.R., Hiddink, J.G., Hinz, H., 2012. Linking temperate demersal fish species to habitat:
643 scales, patterns and future directions. *Fish. Fish.* 14, 256-280.
- 644 Jones, E.G., Tselepidis, A., Bagley, P.M., Collins, M.A., Priede, I.G., 2003. Bathymetric distribution of some
645 benthic and benthopelagic species attracted to baited cameras and traps in the deep eastern Mediterranean.
646 *Mar. Ecol. Prog. Ser.* 251, 75-86.
- 647 Kidawa, A., 2001. Antarctic starfish, *Odontaster validus*, distinguish between fed and starved conspecifics. *Polar.*
648 *Biol.* 24, 408-410.
- 649 King, N.J., Bagley, P.M., Priede, I.G., 2006. Depth zonation and latitudinal distribution of deep-sea scavenging
650 demersal fishes of the Mid-Atlantic Ridge, 42 to 53 degrees N. *Mar. Ecol. Prog. Ser.* 319, 263-274.
- 651 King, N.J., Jamieson, A.J., Bagley, P.M., Priede, I.G., 2008. Deep-sea scavenging demersal fish fauna of the Nazare
652 Canyon system, Iberian coast, north-east Atlantic Ocean. *J. Fish. Biol.* 72, 1804-1814.
- 653 Lampitt, R.S., Merrett, N.R., Thurston, M.H., 1983. Interrelations of necrophagous amphipods, a fish predator, and
654 tidal currents in the deep-sea. *Mar. Biol.* 74, 73-78.
- 655 Langlois, T.J., 2006. Baited underwater video for assessing reef fish populations in marine reserves. *SPC Newsletter*
656 118, 53-57.
- 657 Langlois, T.J., Fitzpatrick, B.R., Fairclough, D.V., Wakefield, C.B., Hesp, S.A., McLean, D.L., Harvey, E.S.,
658 Meeuwig, J.J., 2012. Similarities between line fishing and baited stereo-video estimations of length-
659 frequency: Novel application of kernel density estimates. *Plos One* 7, e45973-e45973.
- 660 Langlois, T.J., Harvey, E.S., Fitzpatrick, B., Meeuwig, J.J., Shedrawi, G., Watson, D.L., 2010. Cost-efficient
661 sampling of fish assemblages: comparison of baited video stations and diver video transects. *Aquat. Biol.* 9,
662 155-168.
- 663 Malcolm, H.A., Gladstone, W., Lindfield, S., Wraith, J., Lynch, T.P., 2007. Spatial and temporal variation in reef
664 fish assemblages of marine parks in New South Wales, Australia - baited video observations. *Mar. Ecol.*
665 *Prog. Ser.* 350, 277-290.
- 666 McLean, D.L., Harvey, E.S., Fairclough, D.V., Newman, S.J., 2010. Large decline in the abundance of a targeted
667 tropical lethrinid in areas open and closed to fishing. *Mar. Ecol. Prog. Ser.* 418, 189-199.

- 668 Meager, J.J., Batty, R.S., 2007. Effects of turbidity on the spontaneous and prey-searching activity of juvenile
669 Atlantic cod (*Gadus morhua*). Philos. Trans. R. Soc. Lond. B. Biol. Sci. 362, 2123-2130.
- 670 Moore, C.H., Harvey, E.S., Van Niel, K., 2010. The application of predicted habitat models to investigate the spatial
671 ecology of demersal fish assemblages. Mar. Biol. 157, 2717-2729.
- 672 Priede, I.G., Bagley, P.M., 2000. In situ studies on deep-sea demersal fishes using autonomous unmanned lander
673 platforms. Oceanog. Mar. Biol. 38, 357-392.
- 674 Priede, I.G., Bagley, P.M., Smith, A., Creasey, S., Merrett, N.R., 1994. Scavenging deep demersal fishes of the
675 Porcupine Seabright, Northeast Atlantic - Observations by baited camera, trap and trawl. J. Mar. Biol.
676 Assoc. UK. 74, 481-498.
- 677 Priede, I.G., Merrett, N.R., 1996. Estimation of abundance of abyssal demersal fishes; A comparison of data from
678 trawls and baited cameras. J. Fish. Biol. 49, 207-216.
- 679 Priede, I.G., Smith, K.L., Armstrong, J.D., 1990. Foraging behaviour of abyssal grenadier fish. Inferences from
680 acoustic tagging and tracking in the North Pacific Ocean. Deep. Sea. Res. 37, 81-101.
- 681 Reidenbach, M.A., Koehl, M., 2011. The spatial and temporal patterns of odors sampled by lobsters and crabs in a
682 turbulent plume. J. Exp. Biol. 214, 3138-3153.
- 683 Sainte-Marie, B., Hargrave, B.T., 1987. Estimation of scavenger abundance and distance of attraction to bait. Mar.
684 Biol. 94, 431-443.
- 685 Saltelli, A., Chan, K., Scott, E.M., 2000. Sensitivity analysis. New York, Wiley.
- 686 Sigler, M.F., 2000. Abundance estimation and capture of sablefish (*Anoplopoma fimbria*) by longline gear. Can J
687 Fish. Aquat. Sci. 57, 1270-1283.
- 688 Smale, D.A., Barnes, D.K.A., Fraser, K.P.P., Mann, P.J., Brown, M.P., 2007. Scavenging in Antarctica: Intense
689 variation between sites and seasons in shallow benthic necrophagy. J. Exp. Mar. Biol. Ecol. 349, 405-417.
- 690 Stobart, B., Garcia-Charton, J.A., Espejo, C., Rochel, E., Goni, R., Renones, O., Herrero, A., Crec'hriou, R., Polti,
691 S., Marcos, C., Planes, S., Perez-Ruzafa, A., 2007. A baited underwater video technique to assess shallow-
692 water Mediterranean fish assemblages: Methodological evaluation. J. Exp. Mar. Biol. Ecol. 345, 158-174.
- 693 Stoner, A., 2004. Effects of environmental variables on fish feeding ecology: implications for the performance of
694 baited fishing gear and stock assessment. J. Fish. Biol. 65, 1445-1471.
- 695 Stoner, A.W., Ryer, C.H., Parker, S.J., Auster, P.J., Wakefield, W.W., 2008. Evaluating the role of fish behavior in
696 surveys conducted with underwater vehicles. Can. J. Fish. Aquat. Sci. 65, 1230-1243.
- 697 Taylor, M.D., Baker, J., Suthers I.M., 2013. Tidal currents, sampling effort and baited remote underwater video
698 (BRUV) surveys: Are we drawing the right conclusions? Fish. Res. 140, 96-104.
- 699 Watson, D.L., Anderson, M.J., Kendrick, G.A., Nardi, K., Harvey, E.S., 2009. Effects of protection from fishing on
700 the lengths of targeted and non-targeted fish species at the Houtman Abrolhos Islands, Western Australia.
701 Mar. Ecol. Prog. Ser. 384, 241-249.
- 702 Watson, D.L., Harvey, E.S., Fitzpatrick, B.M., Langlois, T.J., Shedrawi, G., 2010. Assessing reef fish assemblage
703 structure: how do different stereo-video techniques compare? Mar. Biol. 157, 1237-1250.
- 704 Westera, M., Lavery, P., Hyndes, G., 2003. Differences in recreationally targeted fishes between protected and
705 fished areas of a coral reef marine park. J. Exp. Mar. Biol. Ecol. 294, 145-168.
- 706 Willis, T.J., Babcock, R.C., 2000. A baited underwater video system for the determination of relative density of
707 carnivorous reef fish. Mar. Freshwater. Res. 51, 755-763.

708 Willis, T.J., Millar, R.B., Babcock, R.C., 2003. Protection of exploited fish in temperate regions: High
709 density and biomass of snapper *Pagrus auratus* (Sparidae) in northern New Zealand marine
710 reserves. J. Appl. Ecol. 40, 214-227.

Figure 1

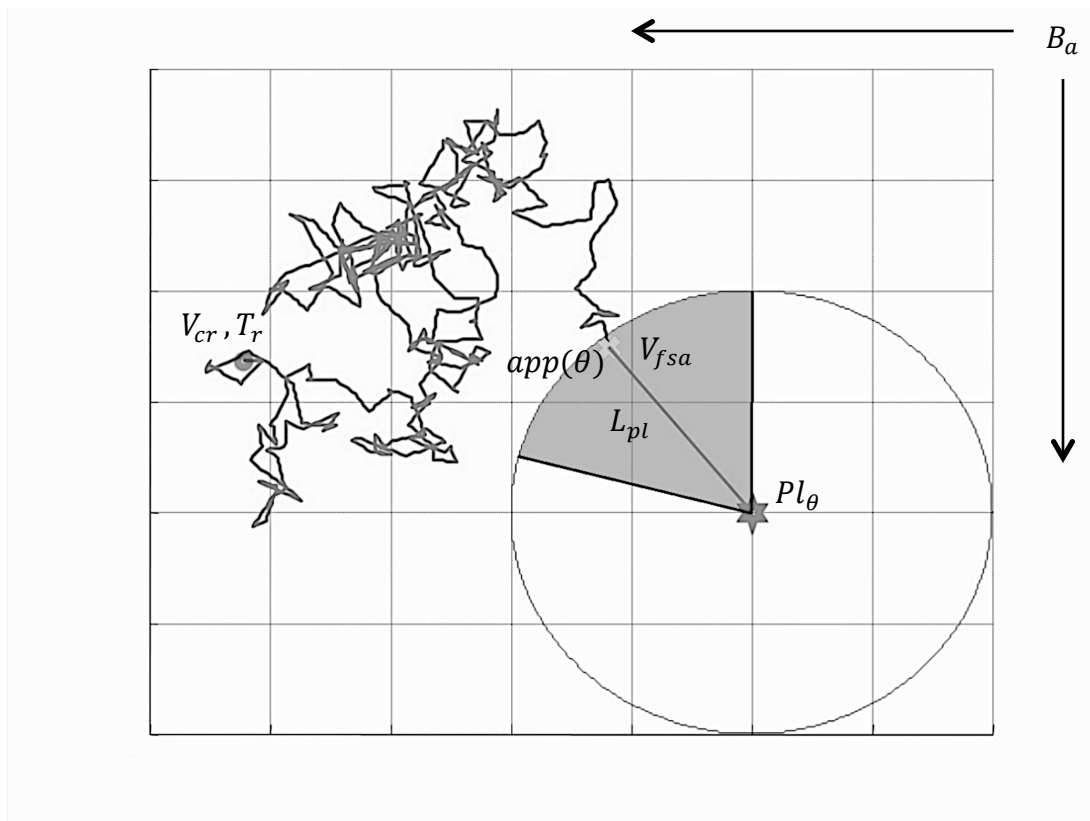


Figure 2

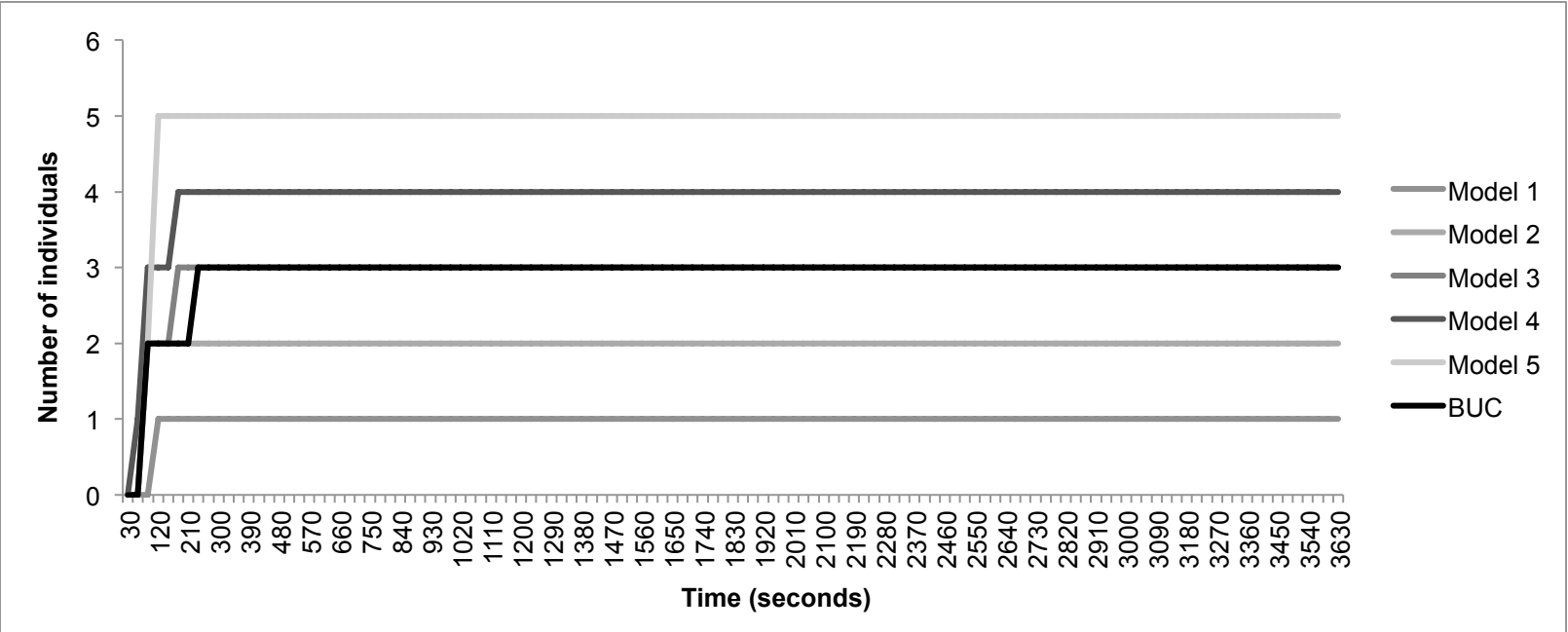
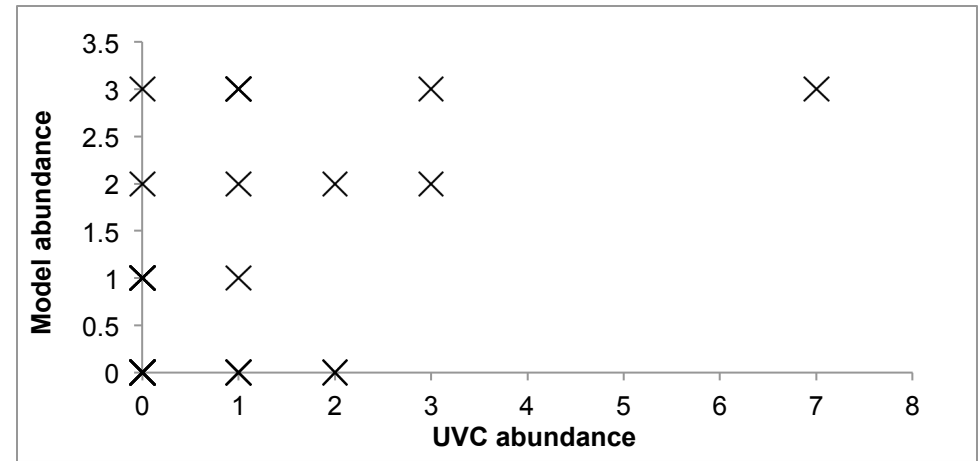
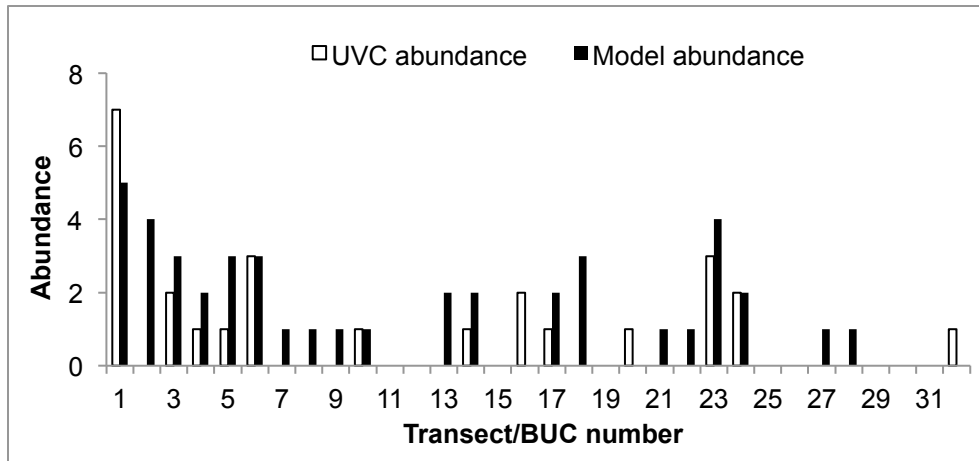
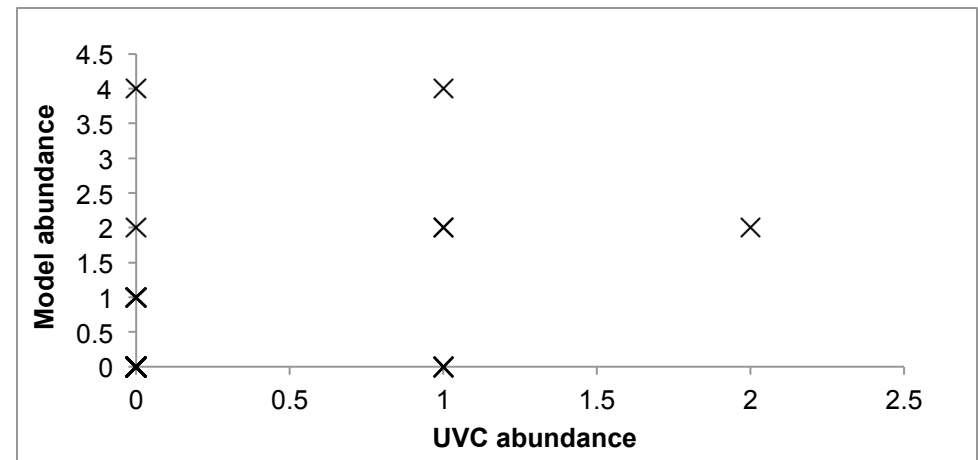
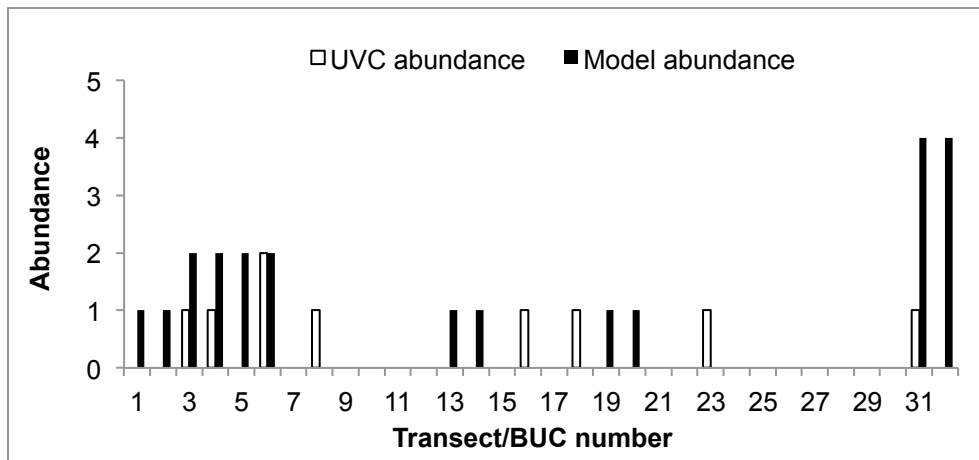


Figure 3

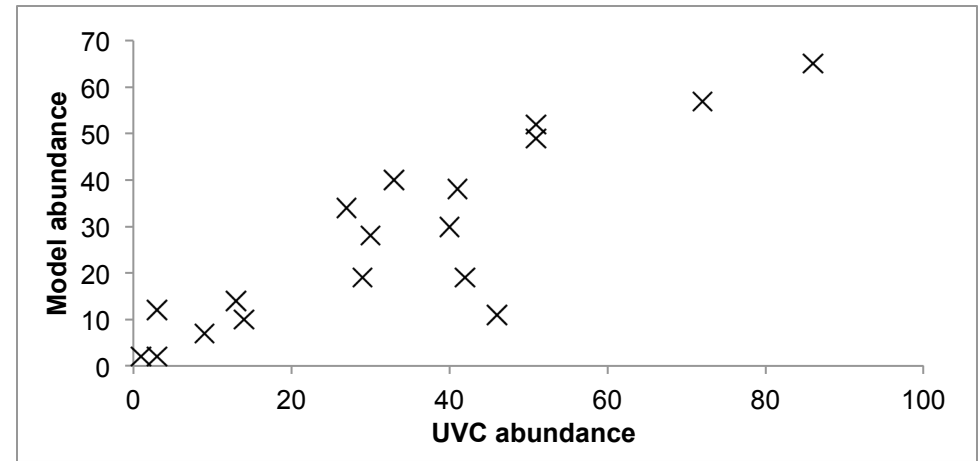
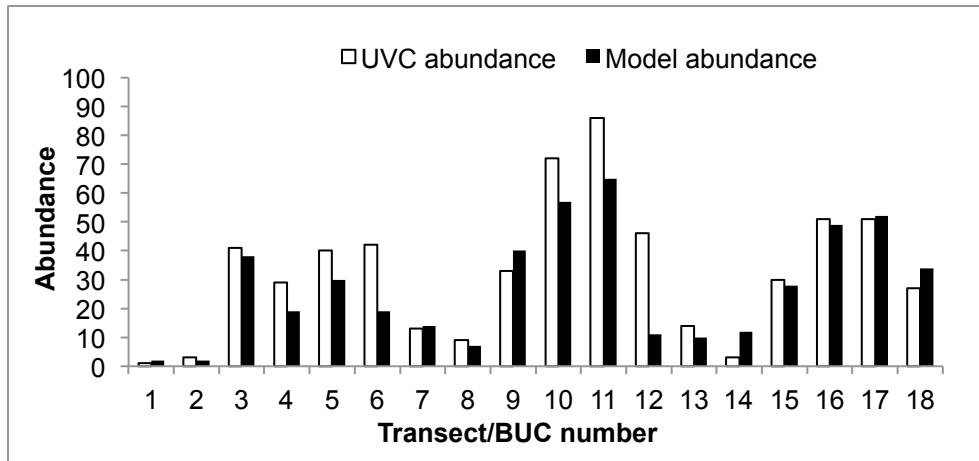
a) *Epinephelus fasciatus*



b) *Gymnothorax* spp.



c) *Odontaster validus*



d) *Parabolasia corrugatus*

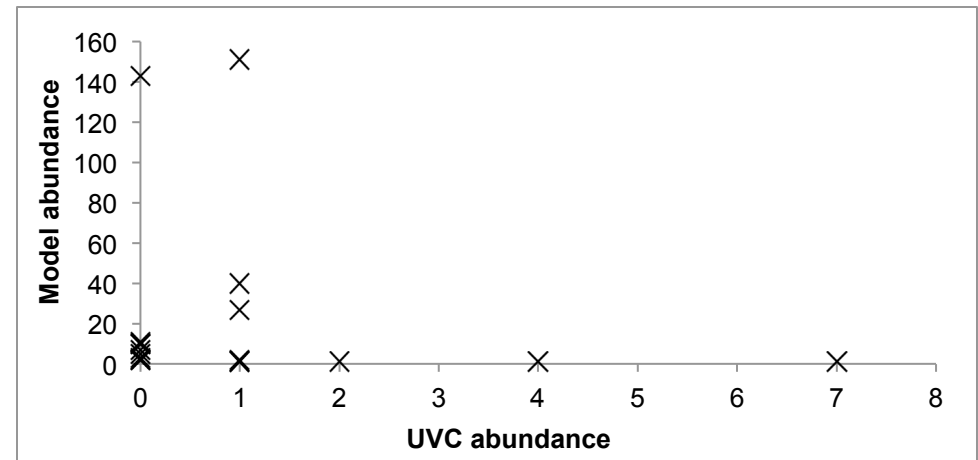
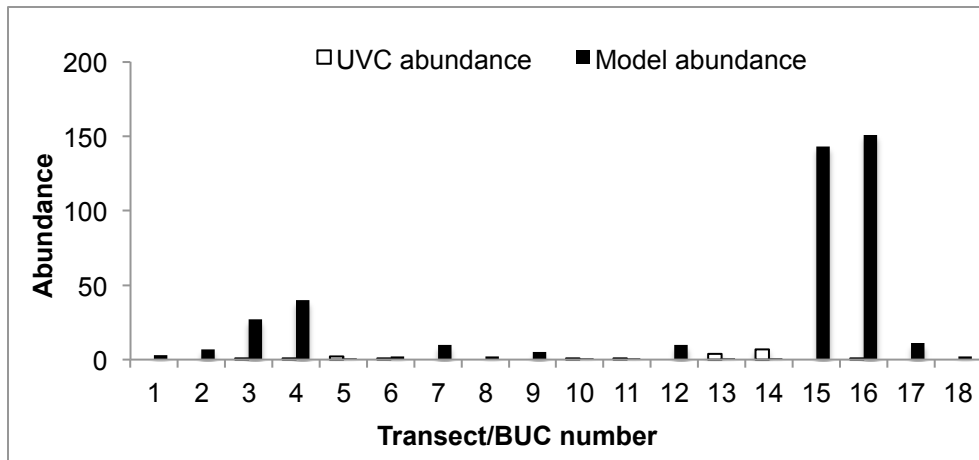
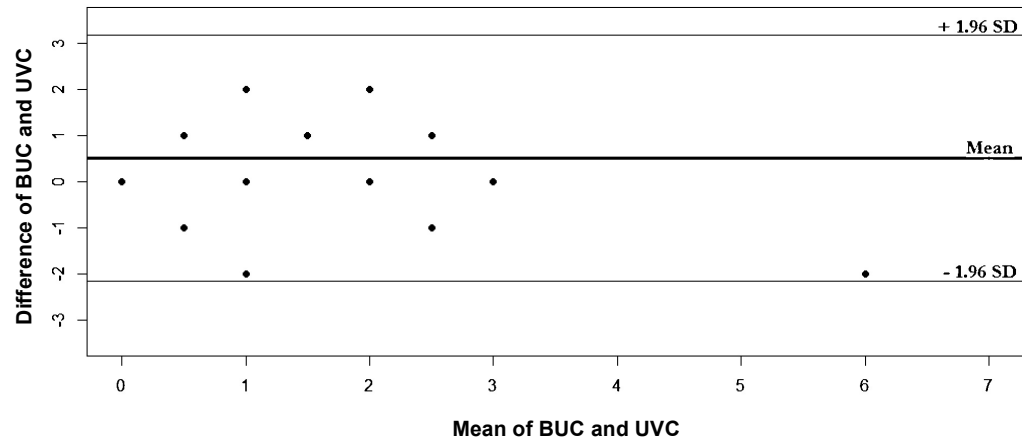
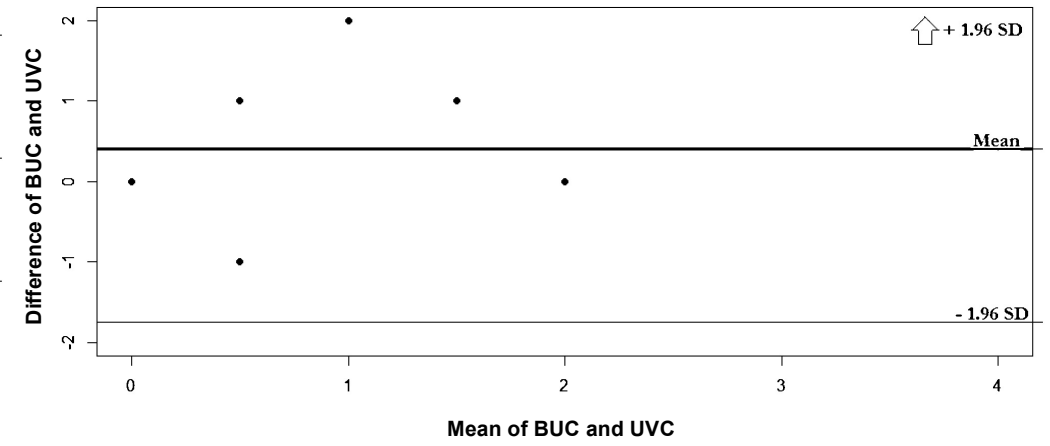


Figure 4

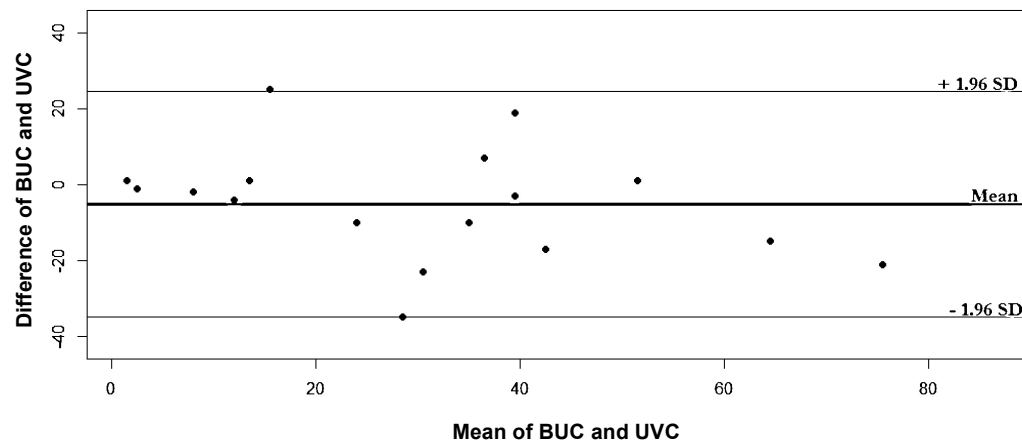
A



B



C



D

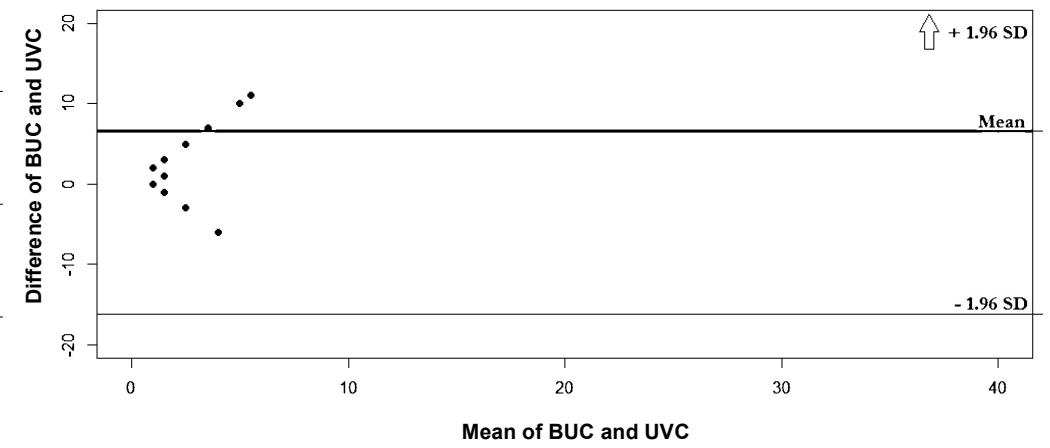


Table 1

Parameters	Area (m ²)	Current speed (m s ⁻¹)	Abundance (individuals)	Cruising speed (m s ⁻¹)	Turning interval (s)	Approach speed (m s ⁻¹)	Staying time (s)	References
Species								
<i>Epinephelus fasciatus</i>	1000	0.02 - 0.2	1 - 100	0 – 0.2	0 - 120	0.294 - 0.365	0 - 240	Fulton, 2007; Bshary et al., 2006
<i>Gymnothorax</i> spp.	1000	0.02 - 0.2	1 - 100	0	0 - 120	0.0935 - 0.318	0 - 180	D'Aout and Aerts, 1999; Gibran, 2007
<i>Odontaster validus</i>	6.25	0.01 - 0.1	1 - 100	0	n/a	0.0001 – 0.001	To simulation end	Kidawa, 2001
<i>Parbolasia corrugatus</i>	6.25	0.01 – 0.1	1 - 100	0	n/a	0.0001 – 0.0003	To simulation end	Clarke and Prothero-Thomas, 1997

